

Magnesium Anthracene Systems, 10<sup>[ $\diamond$ ]</sup>

## Nanocrystalline Zintl Phases from Main-Group Metal Chlorides and Magnesium Anthracene or Activated Magnesium

Ingo Abraham, Lorraine E. Aleandri, Borislav Bogdanović\*, Uwe Kolb, Martin Lagarden, and Klaus Schlichte

Max-Planck-Institut für Kohlenforschung,  
Kaiser-Wilhelm-Platz 1, D-45470 Mülheim an der Ruhr, Germany  
Fax: (internat.) + 49(0)208/306-2980  
E-mail: bogdanovic@mpi-muelheim.mpg.de

Received April 14, 1998

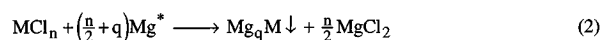
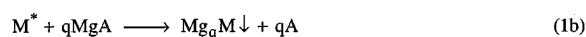
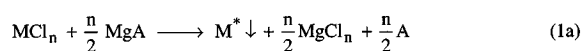
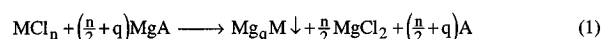
**Keywords:** Magnesium anthracene / Active magnesium / Zintl phases / Magnesium intermetallics / EXAFS spectroscopy

Ga, Tl, Sn, Pb, As, Sb, Bi, Cd, and Hg chlorides react with magnesium anthracene · 3 THF (MgA), anthracene-activated magnesium, or “active magnesium” (Mg\*) in THF, generating the respective Mg intermetallics in a nanocrystalline or amorphous state (Eqs. 1–3). Mg intermetallics accessible through the wet-chemical route can be exploited by

metathetical exchange reactions for the preparation of other, highly active intermetallics and alloys; EXAFS investigation of X-ray amorphous Cu–Sn and Pd–Pb solids thus prepared (Eqs. 13 and 14) shows that they are true bimetallic alloys (solid solutions).

### Introduction

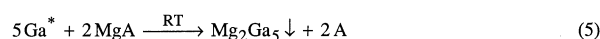
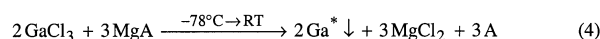
In recent publications<sup>[1]</sup> we have reported the preparation of a series of so-called inorganic Grignard reagents from transition-metal chlorides and organomagnesium compounds or “active magnesium” (Mg\*). These soluble systems can be used as reagents for the synthesis of intermetallics and alloys in a finely divided, usually nanoparticulate, state<sup>[1]</sup>. In contrast to transition-metal chlorides, it was found<sup>[1b]</sup> that chlorides of heavier group 12–15 metals (MCl<sub>n</sub>) in THF react with magnesium anthracene · 3 THF<sup>[2]</sup> (MgA), Mg\*, or ordinary magnesium powder in the presence of catalytic amounts of MgA<sup>[3]</sup>, with formation of magnesium intermetallics (Mg<sub>q</sub>M), also in a finely divided, highly active state<sup>[4]</sup>; the reactions can be described by eqs. 1–3. When MgA is used as the reducing agent (Eq. 1), the reaction progress can be monitored by measuring the increase in anthracene (A) concentration in the reaction solution with time. In some cases, it is advantageous to run the reaction shown in Eq. 1 in two steps. In the first step, MCl<sub>n</sub> is reduced to the metallic state in a highly active form (M\*, Eq. 1a); subsequently, M\* with additional MgA is transformed into Mg<sub>q</sub>M (Eq. 1b). In the following, we give an account of the preparation, characterization, and possible application of magnesium intermetallics obtained via these routes<sup>[1b][4][5]</sup>.



### Results

#### Mg–Ga and Mg–Tl Intermetallics

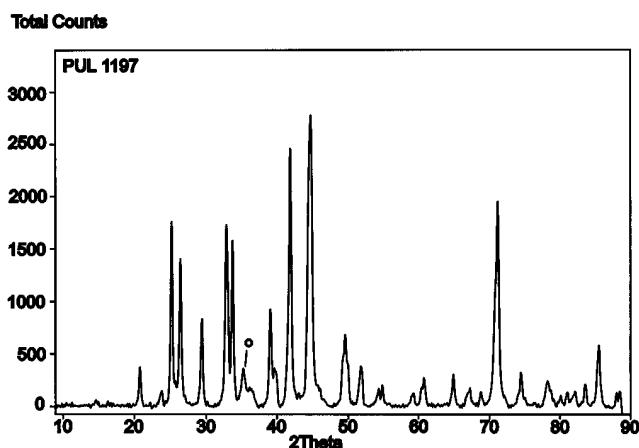
The Ga-rich Zintl phase Mg<sub>2</sub>Ga<sub>5</sub><sup>[6]</sup> has previously been prepared in bulk form by melting stoichiometric mixtures of high-purity Mg and Ga metal sealed in Ta<sup>[6a]</sup> or pyrex crucibles<sup>[6c]</sup>. The preparation of Mg<sub>2</sub>Ga<sub>5</sub> in a finely divided, highly reactive crystalline form can now be achieved via a two-step reaction. In the first step (Eq. 4) GaCl<sub>3</sub> is reduced with MgA at low temperature to give a highly active gallium (Ga\*) suspension in THF. After separating the active metal from MgCl<sub>2</sub> and anthracene, Ga\* can be converted, with additional MgA, into Mg<sub>2</sub>Ga<sub>5</sub> (Eq. 5). Mg<sub>2</sub>Ga<sub>5</sub> is obtained as a black pyrophoric powder contaminated with MgCl<sub>2</sub>, A, and THF (Table 3; Expt. 1).



[ $\diamond$ ] Part 9: R. Benn, B. Bogdanović, M. Brüning, H. Grondey, W. Herrmann, H.-G. Kinzelmann, K. Seevogel, *Chem. Ber.* **1993**, *126*, 225

The XRD pattern of the  $Mg_2Ga_5$  thus prepared (Figure 1) is in accordance with that reported in the literature<sup>[7]</sup>.

Figure 1. X-ray powder diffraction patterns of  $Mg_2Ga_5$ , prepared from  $GaCl_3$  and  $MgA$ ; o, diffraction line of Ga

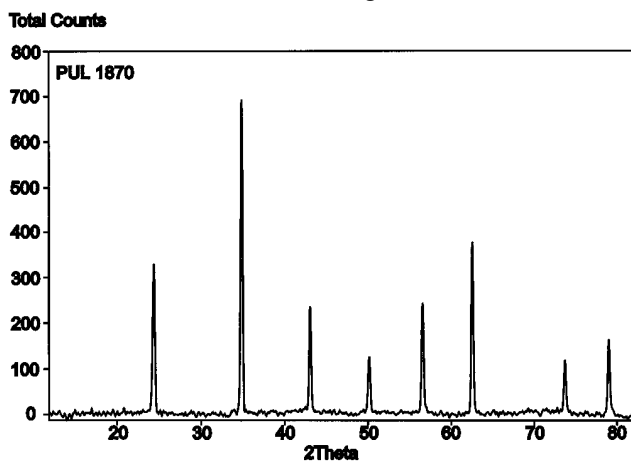


The Mg–Tl Zintl phase  $MgTl$ <sup>[8][9]</sup> can now be prepared in a microcrystalline (nanocrystalline?) form by treating  $TlCl$  with an excess of  $MgA$  in THF (Eq. 6; Expt. 3.2).  $MgTl$  was obtained as a silvery shining powder with the composition  $Mg_{0.88}Tl_{0.01}(CH_2)_{0.2}$ . A DSC analysis of the powder showed a weak endothermic peak at 202.7°C (onset temperature;  $MgTl + Tl$  eutectic; ref.<sup>[10]</sup>, 202°C) and an intense endothermic peak at 351.3°C (onset temperature) corresponding to the melting point of  $MgTl$  (ref.<sup>[10]</sup>, 358°C).



This result, together with the Mg/Tl ratio of 0.88:1 found through elemental analysis, reveals the presence of Tl in the  $MgTl$  thus prepared. However, the XRD powder pattern of this material (Figure 2) exhibited only the diffraction lines of  $MgTl$ <sup>[11]</sup>. The Tl particles if present are, therefore, most likely X-ray amorphous.

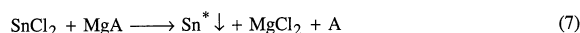
Figure 2. X-ray powder diffraction pattern of  $MgTl$ , prepared from  $TlCl$  and  $MgA$



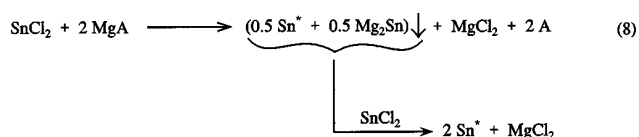
### Mg–Sn and Mg–Pb Intermetallics

Mg forms Zintl phases of the type  $Mg_2E$ ,  $E = Ge, Sn, Pb$ <sup>[8]</sup> with group 14 metals which crystallize in  $CaF_2$  anti-isomorphous structures. Their high melting points reflect the heteropolar character of the bonds between the respective elements. The preparation of  $Mg_2E$  in bulk form has been carried out by melting the components in an inert atmosphere in sealed iron or corundum crucibles<sup>[8][12]</sup>.

The reaction of  $SnCl_2$  with  $MgA$  in THF, as a method for the preparation of Sn or  $Mg_2Sn$ , both in a finely divided state, has been investigated in some detail (Table 4). If the reaction is conducted in the 1:1 molar ratio at room or low temperature (Expts. 4.1 and 4.2), a highly reactive, pyrophoric, black form of metallic Sn of 97–98% purity ( $Sn^*$ , Eq. 7) is obtained.  $Sn^*$  prepared at low temperature (Expt. 4.2) shows only diffuse Sn and no  $Mg_2Sn$  diffraction lines in the XRD spectrum. The high reactivity of  $Sn^*$  prepared according to Eq. 7 is demonstrated by, amongst other things, its reaction with  $MgA$  in THF leading to  $Mg_2Sn$  (see below Eq. 10; Expt. 4.6); commercial Sn powder does not react with  $MgA$  under such conditions.



Reaction of  $SnCl_2$  with  $MgA$  in the molar ratio of 1:2 gives a mixture of  $Sn^*$  and  $Mg_2Sn$  (Expt. 4.3), which, with additional  $SnCl_2$  can again be converted into  $Sn^*$  (Eq. 8).



In order to produce  $Mg_2Sn$  free of  $Sn^*$ , it is necessary to react  $SnCl_2$  with  $MgA$  in an excess amount with respect to Eq. 9 (e.g. in the molar ratio 1:4, Expt. 4.4). The  $Mg_2Sn$  obtained is free of Sn or of the Sn– $Mg_2Sn$  eutectic, according to DSC analysis. The TEM photograph of the  $Mg_2Sn$  thus prepared (Figure 3) reveals aggregates of nonuniform nanocrystals of 10–50-nm size.

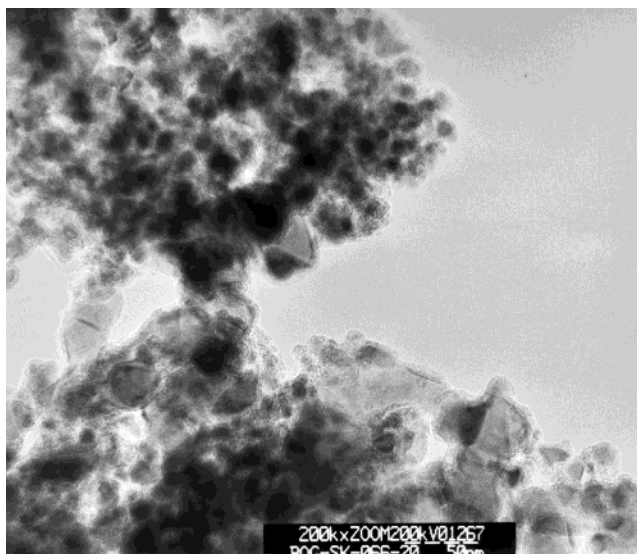


X = Cl, Br

On the basis of the widening of the strongest diffraction line in the XRD of this material, an average particle size of  $40 \pm 4$  nm has been estimated, in agreement with the TEM result.

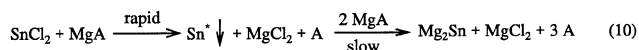
The progress of the reaction of Sn halides with  $MgA$  in the molar ratio of 1:4.1 at 0°C is represented in Figure 4. Under these conditions (Expt. 4.5)  $SnCl_2$  and  $SnBr_2$  yielded  $Mg_2Sn$  with specific surface areas of 70 and 130  $m^2g^{-1}$ , respectively. X-ray powder diffraction showed sharp  $Mg_2Sn$  diffraction lines only.  $SnI_2$  (Figure 4) under the same conditions did not react completely, while hardly any reaction

Figure 3. High-resolution TEM photograph of  $Mg_2Sn$  prepared from  $SnCl_2$  and  $MgA$



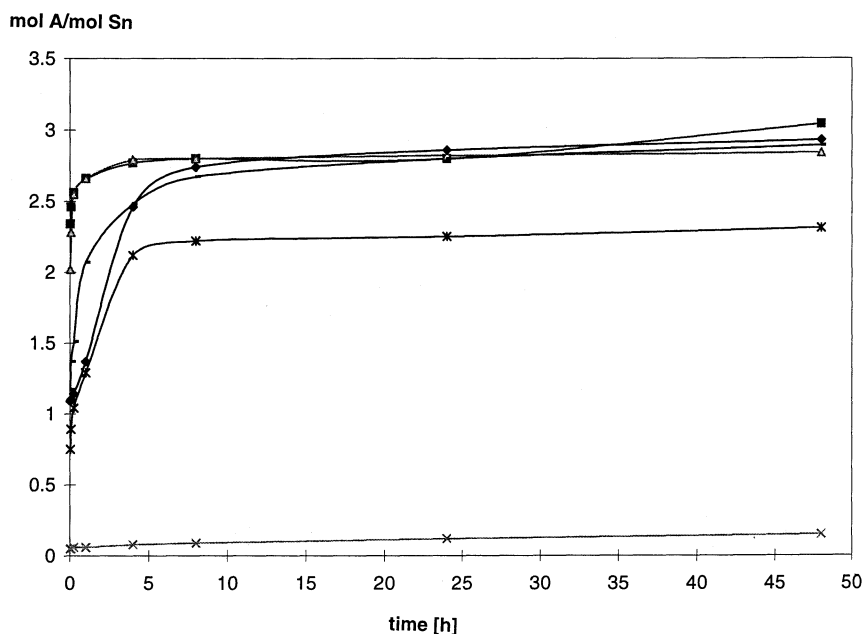
at all was observed with  $SnF_2$ , probably due to the insolubility of  $SnF_2$  and  $MgF_2$  in THF.

$3A/Mg_2Sn$  is, in both cases, only reached after ca. 50 h. The reaction is further slowed down when  $Sn^*$  is separated from  $MgCl_2$  and  $A$  prior to the reaction with additional  $MgA$  (—◆—). Since the reduction of  $SnCl_2$  by  $MgA$  to  $Sn^*$  (Eq. 7) is apparently much more rapid than the conversion of  $Sn^*$  with  $MgA$  in  $Mg_2Sn$ , it is reasonable to assume that  $Sn^*$  also acts as an intermediate in the direct formation of  $Mg_2Sn$  from  $SnCl_2$  and  $MgA$  (Eq. 10). The X-ray diffraction pattern of  $Mg_2Sn$  prepared according to the two-step reaction (Expt. 4.6) is shown in Figure 5.



The preparation of  $Mg_2Pb$  by the wet-chemical method can be carried out by using either stoichiometric amounts of  $MgA$  (Eq. 11) or commercial  $Mg$  powder with  $MgA$  acting as a "phase transfer catalyst" <sup>[11][13]</sup> (Eq. 12). Reaction of  $PbCl_2$  with  $MgA$  in the molar ratio of 1:3.7 in THF (Expt. 5.1) yielded microcrystalline pyrophoric intermetallic  $Mg_2Pb$  which, according to its elemental composition ( $Mg_{1.84}Pb$ ) and X-ray diffractogram, contained minute amounts of  $Pb$ . On the other hand,  $Mg_2Pb$  which was shown using XRD to contain only traces of  $Pb$  (Figure 6)

Figure 4. Progress of the formation reaction of  $Mg_2Sn$  from  $Sn$  halides ( $SnX_2$ ) and  $MgA$  (1:4.1;  $[SnX_2] = 0.06$  mol/l) in THF at  $0^\circ C$ ; —■—,  $SnCl_2$ , one-step reaction; —□—,  $SnCl_2$ , two-step-reaction; —◆—,  $SnCl_2$ , two-step reaction,  $Sn^*$  separated from  $MgCl_2$  and  $A$ ; —▲—,  $SnBr_2$ ; —\*—,  $SnI_2$ ; —×—,  $SnF_2$



The preparation of  $Mg_2Sn$  with a high specific surface area ( $85 \text{ m}^2\text{g}^{-1}$ ) and free of  $Sn^*$  is also possible via the two-step reaction. Accordingly,  $SnCl_2$  is first reacted with  $MgA$  in the molar ratio of 1:1 at room temperature, thus generating  $Sn^*$ , and then at  $0^\circ C$  with 3 additional equivalents of  $MgA$ , giving  $Mg_2Sn$  (Expt. 4.6).

As can further be seen in Figure 4, the rate of the two-step reaction (Expt. 4.6; —□—) is somewhat slower than that of the direct reaction (—■—); but the final ratio of ca.

was obtained by reacting  $PbCl_2$  with  $Mg$  powder and 10 mol-% of  $MgA$  at  $0^\circ C$  (Expt. 5.2).

#### Cu(Mg)–Sn and Pd–Pb Alloys from $Mg_2Sn$ and $Mg_2Pb$ and the Respective Metal Halides

According to preliminary investigations, the highly reactive  $Mg$  intermetallics accessible by the wet-chemical route

Figure 5. X-ray powder diffraction pattern of  $Mg_2Sn$  prepared from  $SnCl_2$  and  $MgA$  in the two-step reaction

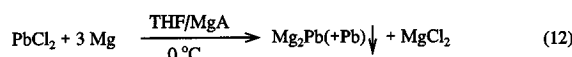
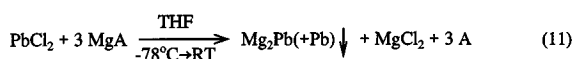
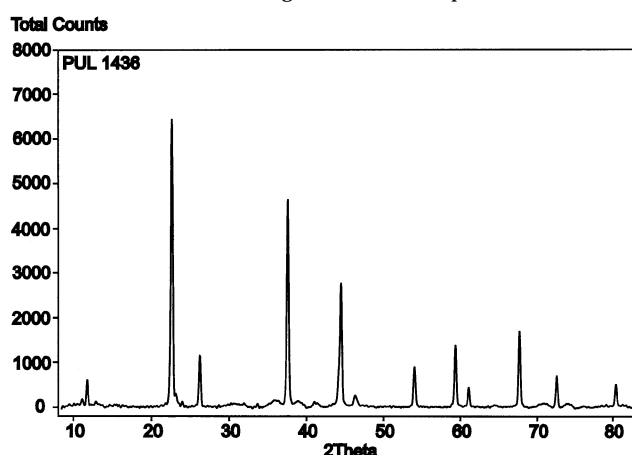
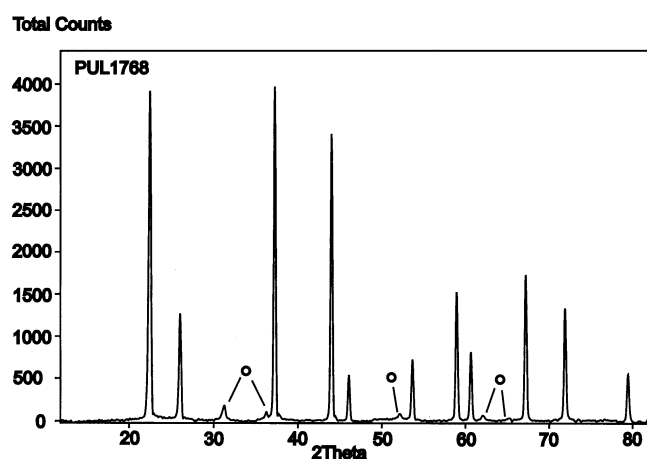


Figure 6. X-ray powder diffraction pattern of  $Pb_2Sn$  prepared from  $PbCl_2$  and  $Mg$  powder in the presence of 10 mol-% of  $MgA$ ; o, diffraction lines of  $Pb$



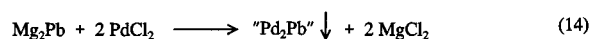
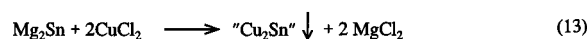
(Eqs. 1–3) can be exploited for the preparation of other intermetallics and alloys in a highly active state. As demonstrated in the following, wet-chemically prepared  $Mg_2Sn$  and  $Mg_2Pb$  react with  $Cu$  and  $Pd$  chlorides, respectively in THF with exchange of  $Mg$  by the metal in question. The reactions can thus be envisaged as a route for the preparation of intermetallics and alloys complementary to that of applying “inorganic Grignard reagents”<sup>[1]</sup> (see Introduction).

$Cu-Sn$ <sup>[14]</sup> and  $Pd-Pb$  alloys<sup>[15]</sup> are accessible via metallurgical methods. A colloidal  $Pd-Pb$  alloy has recently been prepared by Bönnemann et al.<sup>[16]</sup> by means of co-reduction of the corresponding metal salts.  $Pd-Pb$  metal combinations can be used as catalysts for the *cis*-selective hydrogenation of alkynes to alkenes (Lindlar catalyst)<sup>[16][17]</sup>

and for the hydrodechlorination of chlorofluorocarbons (CFCs)<sup>[18]</sup>.

In order to provide starting materials with a high dispersion and reactivity,  $Mg_2Sn$  and  $Mg_2Pb$  utilized for the reactions with metal halides were prepared at low temperatures (Expts. 4.8 and 5.1).  $Mg_2Sn$  prepared at low temperatures (Expt. 4.7) is, indeed, highly dispersed, as demonstrated by its broad but weak diffraction lines in XRD.

Reactions of  $Mg_2Sn$  with  $CuCl_2$  and of  $Mg_2Pb$  with  $PdCl_2$  in the molar ratio of 1:2 (THF, room temperature) gave in quantitative yields solids of the compositions ca.  $Cu_{1.6}Mg_{0.2}Sn(MgCl_2)_{0.1}(CH_2)_{0.4}$  (Expt. 6.1) and ca.  $Pd_{1.9}Pb(MgCl_2)_{0.1}Cl_{0.1}(CH_2)_{0.9}$  (Expt. 6.2), respectively. From the compositions of the solids and the amount of  $Mg^{2+}$  analyzed in THF solutions, it can be concluded that exchange reactions have taken place in the sense of Eqs. 13 and 14. In the first case (Eq. 13), however, these reactions amount only to roughly 80%.



According to the  $Cu-Sn$ <sup>[14]</sup> and  $Pd-Pb$ <sup>[15]</sup> phase diagrams, intermetallic compounds of the compositions  $Cu_2Sn$  and  $Pd_2Pb$  are not known. The X-ray diffractogram for wet-chemically prepared  $Cu(Mg)-Sn$  alloy showed weak diffuse reflections ( $Cu?$ ,  $Sn$ ) only. After heating a sample to 145 or 400 °C, weak diffraction lines for  $Cu_6Sn_5$ <sup>[19]</sup> appeared in the X-ray powder pattern. XRD of the wet-chemically prepared  $Pd-Pb$  alloy showed the presence of  $Pb$ , but upon programmed heating to 300 or 400 °C (in steps of 50 °C), the spectrum showed weak diffraction lines for  $Pd_3Pb$ <sup>[20]</sup>.

In order to gain more information about their structure, both nonannealed X-ray amorphous alloys were investigated using extended X-ray absorption fine structure (EXAFS) spectroscopy.

#### Structural Characterization of the Wet-Chemically Prepared $Cu(Mg)-Sn$ and $Pd-Pb$ Alloys Using EXAFS

The Fourier transforms of the  $k^3\chi(k)$  functions at the  $Cu$ - and  $Sn$ - $K$  absorption edges of the  $Cu(Mg)-Sn$  alloy are dominated by a single peak which at the  $Cu$ - $K$  edge (Figure 7) is markedly split. An adaption of the Fourier-filtered  $k^3\chi(k)$  functions requires, for the  $Sn$  central atom, a single coordination shell of  $Cu$  atoms. For the  $Cu$  central atom, a fit with only a single coordination shell is not possible. Two coordination shells consisting of  $Cu$  and  $Sn$  backscatterers are needed to reproduce the  $Cu$ - $K$  EXAFS spectrum. Although only a limited  $k$  range (3–10 Å<sup>-1</sup>) is available, a clear distinction between  $Cu$  and  $Sn$  backscatterers is possible. Using only  $Cu$  backscatterers, no fit is possible. The structural parameters of the  $Cu(Mg)-Sn$  alloy as determined by EXAFS spectroscopy are summarized in Table 1.

The agreement between the values for the  $Cu-Sn$  distance (2.68 Å) and for the EXAFS Debye-Waller factor  $\sigma$

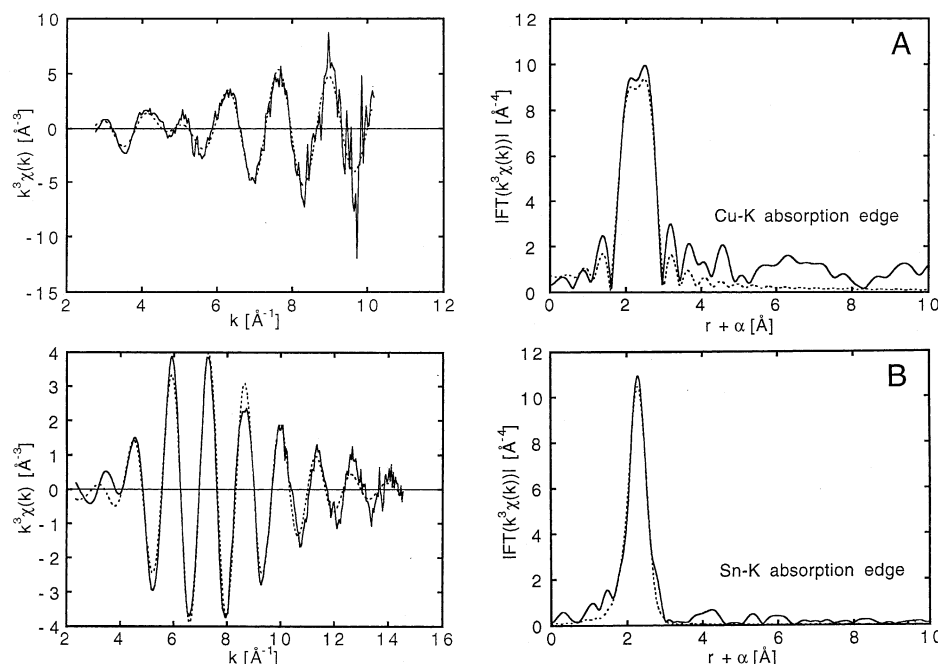
Figure 7. Unfiltered experimental (solid line) and fitted (broken line)  $k^3\chi(k)$  functions and their Fourier transforms of the Cu(Mg)–Sn alloy at the Cu- (A) and Sn-*K* (B) absorption edges

Table 1. Structural parameters of the Cu(Mg)–Sn alloy before annealing determined by EXAFS spectroscopy

absorber	backscatterer	$r$ [Å]	$N$	$\sigma$ [Å]
Sn	Cu	2.68	6.5	0.113
Cu	Sn	2.68	2.6	0.114
	Cu	2.56 <sup>[a]</sup>	2.9	0.098

<sup>[a]</sup> The Cu–Cu distance corresponds to that of the bulk metal.

(0.113 and 0.114) obtained by analysis of the Cu and Sn data shows the structural parameters to be reliable. Although no further-reaching model can be proposed, the structural data (Table 1) allow the following conclusions to be made: (1) for the Sn central atom only Cu backscatterer atoms are observed; the neat Sn phase can therefore only be present to a very low extent, the greatest part of Sn being alloyed with Cu; (2) structural models which postulate the majority of Sn atoms to be on the surface of Cu particles can be excluded because for the Sn central atom ca. 6.5 Cu backscatter atoms are found; (3) the low number of atoms in the coordination shells is characteristic of extremely small metal particles having a large proportion of surface atoms and consisting of no more than a few dozen metal atoms. Coordination numbers determined by EXAFS spectroscopy are influenced by the quality of samples, thus for more accurate determination of coordination numbers further experiments are necessary. This is also especially true for EXAFS investigations of the annealed sample, which exhibit diffractometrically detectable phases and which point to higher coordination numbers; (4) Cu backscatterers at a distance of 2.56 Å are shown to be present

using Cu-*K* EXAFS spectroscopy, demonstrating that a pure Cu phase is present.

The Fourier transforms of the experimental  $k^3\chi(k)$  functions at the Pd-*K* and Pb-*L*<sub>III</sub> absorption edges of the Pb(Mg)Pd alloy also show one single peak with a small shoulder at low  $r$  values. The nonfiltered, experimental and fitted  $k^3\chi(k)$  functions and their Fourier transforms are shown in Figure 8. The curve-fitting procedure shows that the experimental  $k^3\chi(k)$  functions at both the Pd-*K* and at the Pb-*L*<sub>III</sub> absorption edge are dominated by the contribution of Pd backscatterers. Therefore, from the analysis of the Pb-*L*<sub>III</sub> absorption spectrum, it can be concluded that the Pb atoms are mostly alloyed to Pd. Variations of the structural parameters of the Pd backscatterers influence the agreement between nonfiltered, experimental and fitted  $k^3\chi(k)$  functions much more than variations of the structural parameters of the Pb backscatterers.

Both  $k^3\chi(k)$  functions can be reproduced by inclusion of only two coordination shells of Pb and Pd atoms. For the final fits, the EXAFS Debye-Waller factors  $\sigma_{\text{Pb-Pd}}$  and

Table 2. Structural parameters of the Pd–Pb alloy before annealing determined by EXAFS spectroscopy

absorber	backscatterer	$r$ [Å]	$N$	$\sigma$ [Å]
Pb	Pd	2.8	4.2	0.103 <sup>[a]</sup>
	Pb	3.6	1.9	0.144
Pd	Pb	2.8	2.6	0.103 <sup>[a]</sup>
	Pd	2.8	4.6	0.091

<sup>[a]</sup> For the final fits, the EXAFS Debye–Waller factors  $\sigma_{\text{Pb-Pd}}$  and  $\sigma_{\text{Pd-Pb}}$  were constrained to the same value.

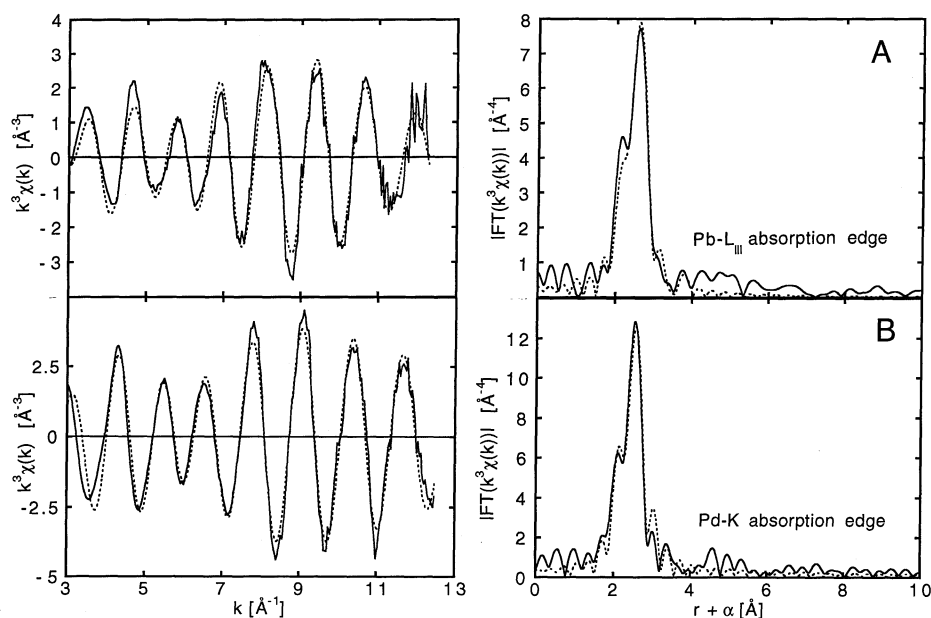
$\sigma_{\text{Pd-Pb}}$  were constrained to the same value. The results of the curve fitting procedures are listed in Table 2.

The agreement between the values for the Pb–Pd distance (2.80 Å) derived from both  $k^3\chi(k)$  functions confirms the reliability of these structural parameters too.

corresponding Zintl phases  $\text{Mg}_3\text{M}_2^*$  in a finely divided, highly active, pyrophoric state (Eq. 16).

$\text{Mg}_3\text{As}_2$  (Expt. 7.1) is obtained by this method as a deep-brown, X-ray amorphous powder, with a specific surface area of  $167.7 \text{ m}^2\text{g}^{-1}$ . After annealing ( $400^\circ\text{C}$ ), the presence

Figure 8. Unfiltered experimental (solid line) and fitted (broken line)  $k^3\chi(k)$  functions and their Fourier transforms for the Pb–Pd alloy at the Pt- $L_{\text{III}}$  (A) and the Pd- $K$  (B) absorption edges

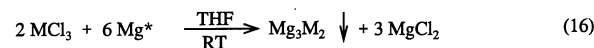
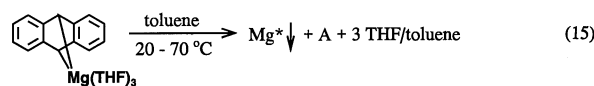


The data allow the following conclusions to be made: (1) only Pd backscatterers can be seen in the first coordination shell of the Pb atoms, suggesting that Pb is predominantly alloyed with Pd and at most a small fraction of Pb atoms exist as a pure Pb phase; (2) Pb atoms contribute significantly to the Pd- $K$  EXAFS spectrum; a considerable part of the Pd atoms are therefore alloyed to Pb atoms; (3) because Pd atoms can also be seen in the first coordination shell of Pd atoms, and the determined Pd–Pd distance of 2.8 Pd Å is close to the Pd–Pd distance in bulk Pd (2.75 Å), a considerable fraction of Pd atoms seem additionally to be present in the form of bulk Pd.

#### Mg–As, Mg–Sb and Mg–Bi Intermetallics

As, Sb and Bi (M) together with Mg form Zintl phases of the formula  $\text{Mg}_3\text{M}_2$ .<sup>[8]</sup>  $\text{Mg}_3\text{As}_2$  has been prepared by Zintl and Huseman<sup>[21]</sup> from As vapour and Mg at elevated temperatures under hydrogen.  $\text{Mg}_3\text{Sb}_2$  and  $\text{Mg}_3\text{Bi}_2$  have been obtained in bulk form by melting stoichiometric mixtures of pure metals in sealed steel crucibles.<sup>[8][21][22]</sup>

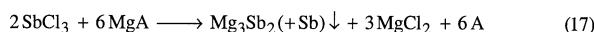
A highly reactive, pyrophoric form of magnesium ( $\text{Mg}^*$ ) with specific surface areas of  $13\text{--}36 \text{ m}^2\text{g}^{-1}$  can be generated by decomposing  $\text{MgA}$  in an organic solvent, such as toluene (Eq. 15).<sup>[23]</sup> By reacting  $\text{AsCl}_3$ , or  $\text{BiCl}_3$  in THF with the  $\text{Mg}^*$  thus obtained, it is possible to prepare the



M = As, Bi

of  $\text{Mg}_3\text{As}_2$  was proved by X-ray diffraction<sup>[24]</sup> (Figure 9).  $\text{BiCl}_3$  reacted with  $\text{Mg}^*$  in THF (Expt. 7.2) to give a black pyrophoric powder with the composition  $\text{Mg}_{1.45}\text{Bi}(\text{MgCl}_2)_{0.06}(\text{CH}_2)_{0.8}$ , whose X-ray diffractogram (without annealing; Figure 10) exhibited strong diffraction lines for  $\text{Mg}_3\text{Bi}_2$ <sup>[25]</sup> and weak ones for Bi.

Reaction of  $\text{SbCl}_3$  with  $\text{MgA}$  in THF (Eq. 17; Expt. 7.3) yielded a highly pyrophoric powder with the composition  $\text{Mg}_{1.49}\text{Sb}(\text{MgCl}_2)_{0.03}(\text{CH}_2)_{1.4}$ . The carbon in the solid was shown to be present in the form of THF and anthracene. An X-ray powder pattern of the sample (Figure 11) after annealing ( $400^\circ\text{C}$ ) demonstrated, however, the presence of a mixture of  $\text{Mg}_3\text{Sb}_2$ <sup>[26]</sup> and Sb.



#### Mg–Cd and Mg–Hg Intermetallics

$\text{CdCl}_2$  reacted with commercial Mg powder (molar ratio 1:2.2) in THF in the presence of catalytic amounts  $\text{MgA}$

Figure 9. X-ray powder diffraction pattern of  $\text{Mg}_3\text{As}_2$ , prepared from  $\text{AsCl}_3$  and  $\text{Mg}^*$  (after annealing,  $400^\circ\text{C}$ )

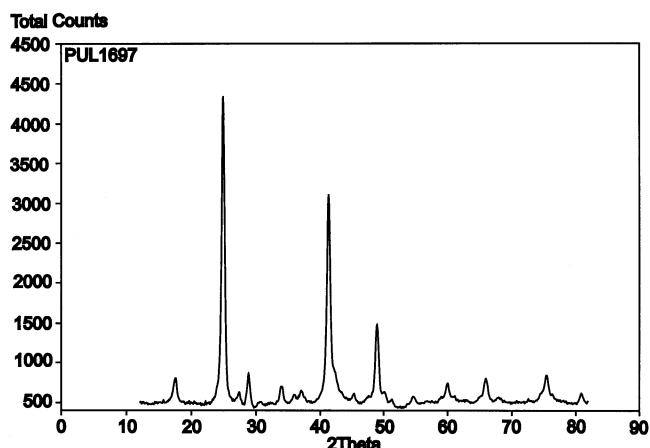


Figure 10. X-ray powder diffraction pattern of  $\text{Mg}_3\text{Bi}_2$ , prepared from  $\text{BiCl}_3$  and  $\text{Mg}^*$ ; o, diffraction lines of Bi

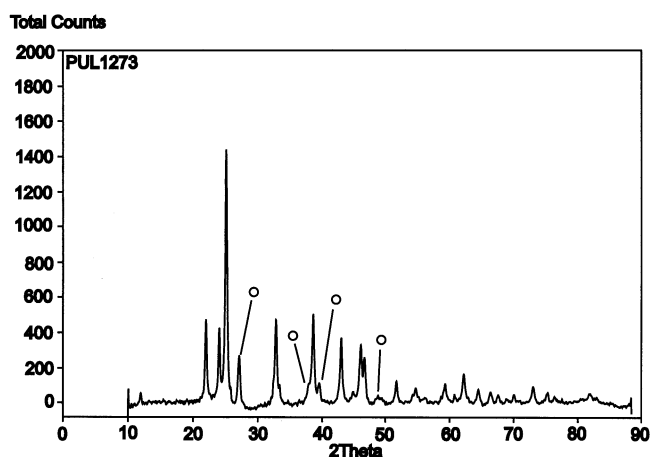
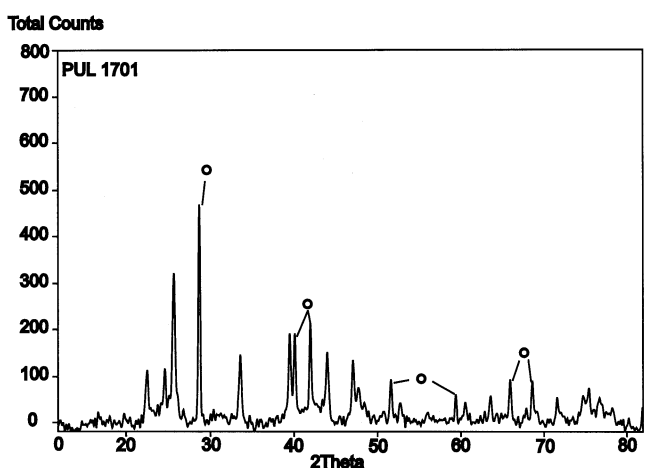


Figure 11. X-ray powder diffraction pattern of  $\text{Mg}_3\text{Sb}_2$  (+ Sb), prepared from  $\text{SbCl}_3$  and  $\text{MgA}$ ; o, diffraction lines of Sb (after annealing,  $400^\circ\text{C}$ )



to give a solid of composition  $\text{Mg}_{1.28}\text{Cd}(\text{MgCl}_2)_{0.02}(\text{CH}_2)_{1.9}$  (Expt. 8.1) which exhibited strong X-ray powder diffraction lines for  $\text{MgCd}$  and a weak reflection for  $\text{MgCd}_3$ <sup>[27]</sup> (Figure 12). The formation of a mixture of  $\text{Mg}-\text{Cd}$  intermetallics

and the presence of ca. 30% of  $\text{Cd}$  in the reaction solution, probably indicate a more complex reaction course than that given by Eq. 18.



The reaction of  $\text{HgCl}_2$  with  $\text{MgA}$  (molar ratio 1:3.8) in THF takes place with a rapid liberation of 2.0 mol anthracene/mol  $\text{HgCl}_2$  and formation of a finely divided solid having the composition  $\text{Mg}_{1.32}\text{Hg}$  (Expt. 8.2); the X-ray powder pattern of the solid exhibited only sharp diffraction lines for  $\text{MgHg}$ <sup>[28]</sup> (Figure 13; Eq. 19).

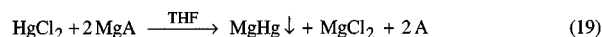


Figure 12. X-ray powder diffraction pattern of  $\text{MgCd}$  (o,  $\text{MgCd}_3$ ), prepared from  $\text{CdCl}_2$  and  $\text{Mg}$  in the presence of 10 mol-% of  $\text{MgA}$

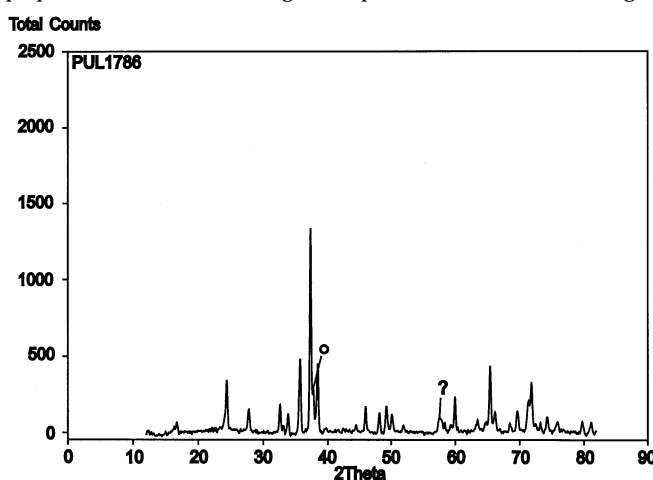
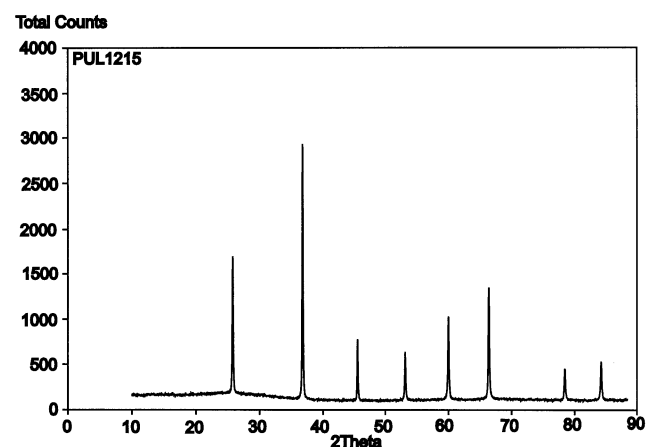


Figure 13. X-ray powder diffraction pattern of  $\text{MgHg}$ , prepared from  $\text{HgCl}_2$  and  $\text{MgA}$



## Conclusion

Magnesium intermetallics with heavier group 12–15 metals, which were previously known only in bulk form<sup>[8]</sup>, can now be prepared in a highly active, nanocrystalline or amorphous state using a wet-chemical method (Eqs. 1–3).

They have, through metathetical exchange reactions (Eqs. 13 and 14), a synthetic potential as reagents for inorganic and organometallic chemistry, especially for the preparation of bimetallic noble metal–main-group metal heterogeneous catalysts<sup>[16][17][18][29][30]</sup>. In this sense, they represent main-group metal counterparts of inorganic Grignard reagents<sup>[1]</sup> (see Introduction). In addition, the low-temperature, kinetically controlled processes, such as for example in Eqs. 13 and 14, may be suitable for the preparation of as yet unknown metastable systems.

The authors thank Prof. Dr. C. Krüger, Dr. C. Lehmann, Dr. B. Tesche, and their coworkers (Max-Planck-Institut für Kohlenforschung) for conducting and discussing the XRD, DSC, TEM, and EDX analyses, and Dr. J. S. Bradley for useful comments. Financial support by the *Fonds der Chemischen Industrie* is gratefully acknowledged.

## Experimental Section

**Instruments:** X-ray diffraction patterns: STOE, STAD/2/PL powder diffractometer, Cu- $K_{\alpha 1}$  radiation; the samples were filled into glass capillaries. HREM images: field emission TEM, Hitachi HF 2000, 200 keV. DSC: DuPont 9900; four points temperature and heat calibration method; heating rate, 10°C/min; Al crucible. EX-AFS<sup>[31]</sup> spectra were recorded at station 9.2 at the SRS, Daresbury using a Si(220) double-crystal monochromator (storage-ring conditions: ca. 2.0 GeV, 150–200 mA). In all cases, data were collected in transmission mode. For the measurements, the material was mixed with PE and pressed to form self-supporting wafers. During the experiments the samples were kept under argon. To eliminate higher harmonics the second monochromator crystal was detuned, reducing the intensity of the X-ray beam to 65% (Pd- $K$  and Sn- $K$  absorption edges) or 50% (Pb- $L_{III}$ , Cu- $K$  absorption edges) of its maximum value. During the experiments, the energy calibration of the monochromator was checked with metal foils. Photoelectron threshold energies of 24350 eV, 29202 eV, 13055 eV, and 8981 eV were chosen for the Pd- $K$ , Sn- $K$ , Pb- $L_{III}$  and Cu- $K$  absorption edges, respectively. Data evaluation was performed in  $k$  space using the program package<sup>[32]</sup> and amplitude and phase data calculated with the program FEF6<sup>[33]</sup>. The usable  $k$  ranges were 2.9–10.2 Å<sup>-1</sup> at the Cu- $K$  edge, 2.4–14.3 Å<sup>-1</sup> at the Sn- $K$  edge, 2.8–12.2 Å<sup>-1</sup> at the Pb- $L_{III}$  edge and 2.4–12.3 Å<sup>-1</sup> at the Pd- $K$  edge.

**Analyses:** Elemental analyses and AAS measurements: Dornis and Kolbe, Mülheim an der Ruhr, Germany.

**Materials:** Magnesium anthracene · 3 THF (MgA).<sup>[2]</sup> Mg powder (270 mesh, PK-31), purchased from the Eckart-Werke, Fürth, Germany, was used in all experiments unless otherwise stated. THF was boiled for several hours over MgA<sup>[2]</sup> and subsequently distilled under argon. All experiments and manipulations with air-sensitive materials were performed under dry argon. Vacuum = 0.1–0.2 mbar; high vacuum = 10<sup>-3</sup> mbar.

**Two-Step Preparation of Mg<sub>2</sub>Ga<sub>5</sub> – Active Gallium (Ga\*) from GaCl<sub>3</sub> and MgA (Expt. 3.1):** 13.0 g (31 mmol) of MgA was suspended in 50 ml of THF. 50 ml of a 0.45 M solution of GaCl<sub>3</sub> in THF (22.5 mmol; GaCl<sub>3</sub> solutions in THF must be stored at ≤ -20°C, because at room temperature the solution eventually solidifies due to cationic polymerisation of THF) was added over a period of 0.5 h into the stirred MgA suspension previously cooled to -78°C. The colour of the suspension changed from orange to a dark brownish black. The stirred suspension was allowed to warm

up to room temperature over a period of 18 h to give a black suspension. The Ga\* was allowed to settle on the bottom of the flask and the green- or yellow-coloured supernatant liquid was removed. The solid was washed with several portions of fresh THF until the supernatant liquid was colourless. The metal could also be isolated by separating the reaction slurry using a centrifuge and, after washing, transferring the solid suspended in fresh THF, into a Schlenk flask.

**Mg<sub>2</sub>Ga<sub>5</sub> from Ga\* and MgA:** 3.67 g (8.7 mmol) of MgA was transferred at room temperature to the Ga\* suspension (see above) in 100 ml of THF. The reaction mixture immediately turned green (reaction of MgA with residual MgCl<sub>2</sub> to form the radical anion complex Mg<sub>2</sub>Cl<sub>3</sub>(THF)<sub>6</sub><sup>+</sup> A<sup>-</sup> ·<sup>[34]</sup>). After stirring at room temperature for 24 h, the product was allowed to settle from the suspension (now dark grey- or black-coloured), washed with several portions of THF, and dried under high vacuum. 1.53 g (83%) of Mg<sub>2</sub>Ga<sub>5</sub> was obtained as a crystalline, black pyrophoric powder. Only diffraction lines corresponding to Mg<sub>2</sub>Ga<sub>5</sub><sup>[7]</sup> were noted in the X-ray powder diffraction pattern (Figure 1).

**MgTI from TiCl and MgA (Expt. 3.2):** Solid TiCl (1.18 g, 4.92 mmol) was added in small portions to a stirred suspension of MgA (15.0 mmol) in THF (100 ml) at room temperature. From time to time 1.0-ml samples were taken from the stirred suspension, quenched with 3.0 ml of a toluene/CH<sub>3</sub>OH mixture (25:1 vol./vol.) containing a known amount of *n*-C<sub>16</sub>H<sub>34</sub> as an internal standard and the content of A in quenched samples determined by GC. Dependence of the concentration of A in solution (mol A/mol TI) from the reaction time (h): 0.21(0.17), 0.43(1.0), 1.29(8), 1.37(24), 1.52(120).

After 170 h, the black suspension was filtered, the precipitate washed several times with THF (until the washing liquids become colourless) and dried in vacuum. MgTI (0.95 g, 81%) was obtained as a silvery shining powder. For the discussion of the DSC analysis of MgTI, see the general section. The X-ray diffractogram of MgTI is shown in Figure 2.

**Sn\* from SnCl<sub>2</sub> and MgA at Room Temperature (Expt. 4.1):** To a cooled and stirred suspension of 6.45 g (15.4 mmol) of MgA in 50 ml of THF was added, in one portion, a solution of 3.21 g (16.9 mmol) of anhyd. SnCl<sub>2</sub> in 50 ml of THF; the temperature of the reaction mixture rose from 13 to 25°C and a black solid precipitated. During the subsequent stirring of the reaction mixture at room temperature, samples (2 ml) of the solution were taken, and by complexometric titration it was determined that the deposition of tin had already been completed after about 3 min. After this time, upon the hydrolysis of an aliquot of the solution, a molar ratio of A/9,10-dihydroanthracene (DHA) of 30:1 was determined by GC. The suspension was filtered, the precipitate was washed with THF and dried under vacuum. 1.34 g of a black powder was obtained which had the composition and the specific surface area as given in Table 4.

**Sn\* from SnCl<sub>2</sub> and MgA at Low Temperatures (Expt. 4.2):** A cooled (ca. -30°C) solution of SnCl<sub>2</sub> in THF was added to a stirred suspension of MgA in THF which had been cooled to -70°C. The suspension was allowed to warm up to room temperature (24 h) and thereafter stirred at room temperature for another 24 h. A small part of Sn\* was isolated by filtration, washing with THF and drying under vacuum. The Sn\* thus obtained exhibited in XRD only broad, diffuse diffraction lines for Sn.

**Preparation of the Sn\*/Mg<sub>2</sub>Sn = 1:1 Mixture from SnCl<sub>2</sub> and MgA and the Subsequent Reaction of the Mixture with SnCl<sub>2</sub> to give Sn\* (Expt. 4.3):** To a stirred solution/suspension of 6.94 g (16.6

Table 3. Mg<sub>2</sub>Ga<sub>5</sub> and MgTl from MCl<sub>n</sub> (M = Ga, Tl) and MgA

expt.	MCl <sub>n</sub> [g] [mmol]	MgA [mmol]	MCl <sub>n</sub> /MgA molar ratio	THF	react. temp. [°C]/ solid react. time [h]	elem. composition [%] Mg M Cl C H empirical formula	yield <sup>[a]</sup> [%]	DSC	XRD
1	GaCl <sub>3</sub> 3.96 (22.5)	31.0	1:1.38	100	-78/0.5 -78 → r. t./18				
		8.7	0:0.39		r. t./24	1.53	13.7 85.1 0.17 0.61 0.30 83 Mg <sub>2.31</sub> Ga <sub>5</sub> Cl <sub>0.02</sub> C <sub>0.2</sub> H <sub>1.2</sub>	n.d.	Mg <sub>2</sub> Ga <sub>5</sub> (Figure 1)
2	TlCl 1.18 (4.92)	15.0	1:3	100	r. t./170	0.95	9.0 85.8 0.15 0.91 0.19 81 Mg <sub>0.88</sub> TlCl <sub>0.01</sub> C <sub>0.2</sub> H <sub>0.5</sub>	see text	MgTl (Figure 2)

<sup>[a]</sup> Based on M.

mmol) of MgA in 50 ml of THF was added dropwise a solution of 1.56 g (8.2 mmol) of anhydrous SnCl<sub>2</sub> dissolved in 50 ml of THF at room temperature over a period of 1 h, whereupon a black suspension formed. After stirring at room temperature for 1 h, a 2-ml sample of the suspension was protolyzed with 2 ml of a mixture of toluene/CH<sub>3</sub>OH, 25:1, (using *n*-C<sub>16</sub>H<sub>34</sub> as an internal standard) and analyzed by GC, whereafter the batch contained 15.4 mmol of anthracene and 0.3 mmol of 9,10-dihydroanthracene. Analysis of the deep-blue THF solution by complexometry showed 9.4 mmol of Mg<sup>2+</sup> and 0.01 mmol of Sn. The suspension was filtered, and the solid was washed with THF until the washing liquid was colourless. After drying under vacuum, 1.17 g of black pyrophoric solid was obtained which had the composition Mg 12.4, Sn 60.5, C 1.9, H 0.3% (Mg/Sn = 1:1). After hydrolysis (H<sub>2</sub>O + 5 N H<sub>2</sub>SO<sub>4</sub>, 1:1) of a sample of the solid and GC analysis of the organic portion, the solid contained 0.03% of anthracene. According to the X-ray powder analysis the solid was a mixture of Mg<sub>2</sub>Sn with elemental Sn.

The preparation of the 1:1 mixture of Mg<sub>2</sub>Sn + Sn\* was repeated in the same manner as described above and was confirmed by X-ray powder analysis of an isolated small sample of the solid. The moist solid left after filtration was suspended in 50 ml of THF, the stirred suspension was mixed with a solution of 8.2 mmol of SnCl<sub>2</sub> in 47 ml of THF, and the mixture was stirred at room temperature for 7 h. The suspension was filtered and the solid was washed with THF and dried under vacuum. According to the X-ray diffractogram, only Sn, with no Mg<sub>2</sub>Sn, was present in the solid.

*Mg<sub>2</sub>Sn from SnCl<sub>2</sub> and MgA (Expt. 4.4):* 35 ml of a 0.217 M solution of SnCl<sub>2</sub> in THF (7.6 mmol) was added dropwise within 15 min to a stirred suspension of 12.82 g (30.6 mmol) of MgA in 100 ml of THF. (Solutions of SnCl<sub>2</sub> in THF are stable at room temperature for only ca. 15 min, but can be stored for long periods of time at -20°C.) The colour of the suspension changed from orange to olive green-black during the slightly exothermic reaction. After stirring for 3 h, the suspension was filtered (D4 sinter) and the solid washed with ca. 100-ml aliquots of THF. The filtrate was yellow-green (unreacted MgA) and at the final washing colourless. GC analysis of the combined filtrate showed 25.5 mmol of A and 3.4 mmol of DHA to be present. The black solid was dried under vacuum. Mg<sub>2</sub>Sn (1.39 g, 87%) was obtained as a crystalline, black pyrophoric powder with the composition and the specific surface area as given in Table 4. A DSC analysis of a sample of Mg<sub>2</sub>Sn thus prepared showed no endothermic peak up to 300°C (confirming the absence of Sn, m.p. 231.97°C, or of a Sn-Mg<sub>2</sub>Sn eutectic, m.p. 203.5°C), but a weakly exothermic peak at 219°C. An X-ray diffractogram of a sample of Mg<sub>2</sub>Sn was in accordance with the line diagram of Mg<sub>2</sub>Sn from ref.<sup>[35]</sup>.

The TEM photograph of Mg<sub>2</sub>Sn taken from the experiment is reproduced in Figure 3; point-by-point EDX analyses of the nanocrystals gave Mg/Sn ratios ranging between 1.7 and 2.7, the majority of analyses giving a value of 2.0. Traces of Cl but no free Mg or Sn could be identified by EDX. The results confirm the formation of the intermetallic Mg<sub>2</sub>Sn.

*Monitoring of the Reaction SnCl<sub>2</sub> and MgA to form Mg<sub>2</sub>Sn at 0°C (Expt. 4.5):* 32.1 mmol of MgA was suspended in 125 ml of THF, the suspension was cooled to 0°C and kept at that temperature throughout the experiment by means of a cryostat. To the stirred suspension were added 1.48 g (7.8 mmol) of solid SnCl<sub>2</sub>. 2.0 ml samples were taken periodically (see Figure 4) from the stirred suspension, quenched with a standard solution (see Expt. 3.2) and the content of A and DHA in the hydrolyzed samples with respect to the standard were determined by GC analysis. Analogous experiments were also carried out with equimolar amounts of SnF<sub>2</sub>, SnBr<sub>2</sub>, and SnI<sub>2</sub>, and the same amounts of MgA and solvent. The results are graphically represented in Figure 4.

*The Two-step Preparation of Mg<sub>2</sub>Sn from SnCl<sub>2</sub> and MgA (Expt. 4.6):* A solution of 7.7 mmol of SnCl<sub>2</sub> in 30 ml of THF was added dropwise to a stirred suspension of 7.7 mmol of MgA in 100 ml of THF. The black suspension of Sn\* was stirred at room temperature for 1 h. The suspension was then cooled down to 0°C and an additional 24.5 mmol of MgA added. The progress of the stirred-batch reaction at 0°C was monitored as described in Expt. 4.5 and is represented graphically in Figure 4. The Mg<sub>2</sub>Sn thus prepared was isolated and analyzed as described for Expt. 4.4; X-ray diffractogram, see Figure 5.

*Mg<sub>2</sub>Sn from SnCl<sub>2</sub> and MgA at Low Temperature (Expts. 4.7 and 4.8):* The experiments were conducted in an analogous manner to Expt. 4.4, except that SnCl<sub>2</sub> was added to MgA each time at -70°C and, thereafter, the temperature of the reaction mixtures slowly raised from -70°C to room temperature (see Table 4). The Mg<sub>2</sub>Sn thus prepared (Expt. 4.7) exhibited in the X-ray diffractogram only broad diffuse reflections characteristic of the intermetallic and Sn. The Mg<sub>2</sub>Sn prepared in Expt. 4.8 was used for the reaction with CuCl<sub>2</sub> to form a Cu-Sn alloy (see Expt. 6.1).

*Mg<sub>2</sub>Pb from PbCl<sub>2</sub> and MgA at Low Temperatures (Expt. 5.1):* The experiment was conducted in the same manner as Expts. 4.7 and 4.8. The XRD powder pattern of the reaction product was consistent with Mg<sub>2</sub>Pb, except for very weak reflections for Pb; Mg<sub>2</sub>Pb thus prepared was used for the reaction with PdCl<sub>2</sub> to form a Pd-Pb alloy (Expt. 6.2).

*Mg<sub>2</sub>Pb from PbCl<sub>2</sub>, Mg Powder and 10 mol-% of MgA (Expt. 5.2):* A suspension of 1.69 g (6.1 mmol) of PbCl<sub>2</sub>, 19.1 mmol of

Table 4. Sn\* and Mg<sub>2</sub>Sn from SnCl<sub>2</sub> and MgA

expt.	SnCl <sub>2</sub> [g] (mmol)	MgA [mmol]	SnCl <sub>2</sub> /MgA molar ratio	THF	react. temp. [°C]/ react. time [h]	solid [g]	<i>elem. composition [%]</i> <i>Mg Sn Cl C H</i> empirical formula	yield <sup>[a]</sup> [%]	sp. surf. area [m <sup>2</sup> g <sup>-1</sup> ]	XRD
1	3.21 (16.9)	15.4	1:0.9	100	r. t./2	1.34	1.2 96.8 0.35 nd Mg <sub>0.06</sub> SnCl <sub>0.01</sub>	65	16.2	nd
2	8.20 (43.3)	40.0	1:0.92	280	-70 → r. t./24 r. t. / 24	0.94 <sup>[b]</sup>	0.57 97.9 0.74 0.44 0.1 Mg <sub>0.03</sub> SnCl <sub>0.02</sub> C <sub>0.04</sub> H <sub>0.1</sub>	nd	nd	Sn
3	1.56 (8.2)	16.6	1:2	100	r. t./1	1.17	12.4 60.5 nd 1.9 0.3 MgSnCl <sub>0.3</sub> H <sub>0.6</sub>	73	nd	Mg <sub>2</sub> Sn <sup>[c]</sup> + Sn
4	1.44 (7.6)	30.6	1:4	135	r. t./3	1.39	26.8 61.8 1.3 8.8 1.1 Mg <sub>2.1</sub> SnCl <sub>0.07</sub> C <sub>1.4</sub> H <sub>2.0</sub>	87	72.8	Mg <sub>2</sub> Sn <sup>[d]</sup>
5	1.48 (7.8)	32.1	1:4.1	125	0/48	1.21	25.4 62.0 1.5 9.4 1.4 Mg <sub>2</sub> SnCl <sub>0.08</sub> C <sub>1.5</sub> H <sub>2.7</sub>	81	70.3	Mg <sub>2</sub> Sn <sup>[e]</sup> (+ Sn)
6	1.44 (7.6)	7.7	1:1	130	r. t./1					
		24.5	0:3.2		0/122	1.21	27.8 63.6 0.75 2.3 0.6 Mg <sub>2.13</sub> SnCl <sub>0.04</sub> C <sub>0.4</sub> H <sub>1.0</sub>	81	85.5	Mg <sub>2</sub> Sn <sup>[e][f]</sup>
7	5.31 (28.0)	97.3	1:3.5	300	-70 → -40/2 -40 → r. t./22	5.32	22.4 59.1 2.1 9.3 1.4 Mg <sub>1.85</sub> SnCl <sub>0.1</sub> C <sub>1.6</sub> H <sub>2.8</sub>	95	54.8	
8	2.49 (13.1)	45.4	1:3.5	220	-70 → r. t./6 r. t./96	<sup>[g]</sup>				

<sup>[a]</sup> Based on Sn. – <sup>[b]</sup> Only a small fraction of the solid was isolated. – <sup>[c]</sup> Reaction with SnCl<sub>2</sub> to give Sn, see text. – <sup>[d]</sup> TEM photograph, see Figure 3. – <sup>[e]</sup> Progression of the reaction with time, see Figure 4. – <sup>[f]</sup> XRD in Figure 5. – <sup>[g]</sup> Not isolated; used for the reaction with CuCl<sub>2</sub> (Expt. 6.1).

Mg powder and 1.9 mmol of MgA in 200 ml of THF was stirred for 10 days at 0 °C. During the first 24 h of reaction the total amount of Mg<sup>2+</sup> analyzed in the THF solution increased to 7.3 mmol and, thereafter, remained constant. Hydrolysis of an aliquot of the THF solution gave 1.5 mmol of *n*-butanol, expressed in terms of the whole solution (GC analysis) – the product of THF cleavage by Mg<sup>[23a]</sup>. Mg<sub>2</sub>Pb was isolated from the THF solution in the same way as described in Expt. 4.4. XRD powder pattern in Figure 6.

*A Cu(Mg)Sn Alloy from Mg<sub>2</sub>Sn and CuCl<sub>2</sub> (Expt. 6.1):* The Mg<sub>2</sub>Sn suspension in THF (Expt. 4.8) was allowed to settle, the green supernatant solution was syphoned off, 50 ml of THF was added to the Mg<sub>2</sub>Sn, the resulting suspension was stirred for 30 min, and the solution was again syphoned off. This operation was repeated two more times. Then, Mg<sub>2</sub>Sn was suspended in 100 ml of fresh THF, the suspension was mixed with 3.48 g (25.9 mmol) of anhydrous CuCl<sub>2</sub> and was stirred at room temperature for 65 h. The black suspension was filtered, the solid was washed 4 or 5

Table 5. Mg<sub>2</sub>Pb from PbCl<sub>2</sub> and MgA or Mg powder and 10 mol-% of MgA

expt.	PbCl <sub>2</sub> [g] (mmol)	MgA or Mg + MgA [mmol]	Pb/Mg ratio	THF	react. temp. [°C]/ react. time [h]	solid [g]	<i>elem. composition [%]</i> <i>Mg Pb Cl C H</i> empirical formula	yield <sup>[a]</sup> [%]	sp. surf. area [m <sup>2</sup> g <sup>-1</sup> ]	XRD
1	4.84 (17.4)	MgA 64.7	1:3.7	300	-78 → r. t./24 r. t./72	4.70	15.3 70.7 1.0 4.5 0.6 Mg <sub>1.84</sub> PbCl <sub>0.08</sub> C <sub>1.1</sub> H <sub>1.8</sub>	92	10.7	Mg <sub>2</sub> Pb <sup>[b]</sup> (+ Pb)
2	1.69 (6.1)	Mg 19.1 + MgA 1.9	1:3.5	200	0/260 <sup>[c]</sup>	1.56	15.6 71.6 0.98 3.3 0.5 Mg <sub>1.86</sub> PbCl <sub>0.08</sub> C <sub>0.8</sub> H <sub>1.4</sub>	90	nd	Mg <sub>2</sub> Pb <sup>[d]</sup> (+ Pb)

<sup>[a]</sup> Based on Pb. – <sup>[b]</sup> Used for the reaction with PdCl<sub>2</sub> (Expt. 6.2). – <sup>[c]</sup> According to the amount of Mg<sup>2+</sup> in the THF solution, the reaction was complete after ca. 20 h. – <sup>[d]</sup> XRD powder pattern in Figure 6.

Table 6. Cu–Sn and Pd–Pb alloys from Mg<sub>2</sub>Sn, Mg<sub>2</sub>Pb and the respective metal chlorides (M'Cl<sub>2</sub>)

expt.	Mg <sub>2</sub> M [g] (mmol)	M'Cl <sub>2</sub> (mmol)	Mg <sub>2</sub> M: M'Cl <sub>2</sub> molar ratio	THF [ml]	react. time <sup>[a]</sup> [h]	solid [g]	<i>elem. composition [%]</i> <i>M' Mg M Cl C H</i> empirical formula	yield <sup>[b]</sup> [%]	sp. surf. area [m <sup>2</sup> g <sup>-1</sup> ]	XRD
1	Mg <sub>2</sub> Sn (13.1)	CuCl <sub>2</sub> (25.9)	1:2	150	65	3.23	41.5 2.4 47.6 1.9 3.6 0.599 Cu <sub>1.64</sub> Mg <sub>0.25</sub> SnCl <sub>0.13</sub> C <sub>0.4</sub> H <sub>1.2</sub>		31.2	Cu <sub>6</sub> Sn <sub>5</sub> + Cu <sub>3</sub> Sn <sup>[c]</sup>
2	Mg <sub>2</sub> Pb (2.14)	PdCl <sub>2</sub> (4.8)	1:2.2	30	170	0.99	44.4 0.6 45.4 2.4 1.4 0.3100 Pd <sub>1.90</sub> Mg <sub>0.12</sub> PbCl <sub>0.31</sub> C <sub>0.9</sub> H <sub>1.4</sub>		18.9	Pd <sub>3</sub> Pb + Pd <sub>3</sub> Pb <sub>2</sub> <sup>[c]</sup>

<sup>[a]</sup> Room temperature. – <sup>[b]</sup> Based on M. – <sup>[c]</sup> After heating the sample to 400 °C.

times with THF and was dried under high vacuum, yielding 3.23 g of an Mg-containing Cu–Sn alloy which had the composition shown in Table 6. The EXAFS spectra of the Cu(Mg)Sn alloy are shown in Figure 7 and discussed in the text. In the filtrate of the batch were found 20.6 mmol of  $\text{Mg}^{2+}$  by way of an analysis (79%).

*A Pd(Mg)Pb Alloy from  $\text{Mg}_2\text{Pb}$  and  $\text{PdCl}_2$  (Expt. 6.2):* 0.85 g (4.8 mmol) of anhydrous  $\text{PdCl}_2$  was added to a stirred suspension of 0.63 g of  $\text{Mg}_2\text{Pb}$  from Expt. 5.1 (2.14 mmoles Pb) in 30 ml of THF. The suspension was stirred for 7 d at room temperature, filtered and the resulting solid washed with THF and dried under high vacuum. Yield: 0.99 g of a black powder of the composition as given in Table 6. The EXAFS spectra of the Pd(Mg)Pb alloy are shown in Figure 8 and discussed in the text.  $\text{Mg}^{2+}$  content of the filtrate: 4.1 mmol.

*$\text{Mg}_3\text{As}_2$  from  $\text{AsCl}_3$  and  $\text{Mg}^*$  (Expt. 7.1):* 9.21 g (22.2 mmoles) of MgA was suspended in 400 ml of toluene and stirred at room temperature for 24 h yielding a fine grey suspension of  $\text{Mg}^*$ . Most of the solvent toluene was removed by decanting leaving ca. 40 ml of toluene with  $\text{Mg}^*$ . After adding 100 ml of THF and 1.30 g (7.15 mmol) of  $\text{AsCl}_3$  to  $\text{Mg}^*/\text{THF}$  suspension, the reaction mixture was stirred for 5 d at room temperature. After filtration, washing with THF and pentane, and drying under vacuum, 0.95 g of  $\text{Mg}_3\text{As}_2$  was obtained as a deep brown pyrophoric powder. XRD powder pattern in Figure 9.

*$\text{Mg}_3\text{Bi}_2$  from  $\text{BiCl}_3$  and  $\text{Mg}^*$  (Expt. 7.2):* The experiment was conducted in the same manner as in Expt. 7.1. XRD powder pattern in Figure 10.

*( $\text{Mg}_3\text{Sb}_2 + \text{Sb}$ ) from  $\text{SbCl}_3$  and MgA (Expt. 7.3):*  $\text{SbCl}_3$  was added to the stirred suspension of MgA in THF. The reaction mixture was stirred for several days at room temperature. The solid was isolated in the same manner as described in Expt. 7.1. After a hydrolytic work-up of the solid, THF and anthracene were identified in the organic phase by mass spectrometry.

*$\text{MgCd} (+ \text{MgCd}_3)$  from  $\text{CdCl}_2$ , Mg Powder and a Catalytic Amount of MgA (Expt. 8.1):* A mixture of 1.33 g (7.24 mmol) of anhydrous  $\text{CdCl}_2$  and 0.38 g (15.8 mmol) of Mg powder in 100 ml of THF was stirred at room temperature for 72 h; during this time, no reaction took place between  $\text{CdCl}_2$  and Mg, as shown by the absence of any  $\text{MgCl}_2$  in the THF solution. After addition of 1.0 mmol of MgA, the mixture was stirred for an additional 48 h, after which 11.0 mmol of Mg in the form of  $\text{MgCl}_2$  (65.4% of the total amount of Mg used) was determined by complexometry in the solution ( $\text{Cd}^{2+}$  ions were masked by addition of KCN). After further stirring for several days, the concentration of  $\text{MgCl}_2$  in the THF solution remained almost unchanged. Filtration, washing with THF and drying under high vacuum yielded 0.91 g of a grey powder with the composition given in Table 8. The X-ray pattern of the powder (Figure 12) exhibited, in addition to one weak signal

Table 7.  $\text{Mg}_3\text{M}_2$  (M = As, Sb, Bi) Zintl phases from  $\text{MCl}_3$  and  $\text{Mg}^*$ , Mg powder or MgA

expt.	$\text{MCl}_3$ [g] (mmol)	$\text{M}^*(\text{Mg})$ or MgA [mmol]	$\text{MCl}_3/\text{Mg}$ molar ratio	THF [ml]	reaction <sup>[a]</sup> time [h]	solid [g]	elem. composition [%] <i>Mg M Cl C H</i> empirical formula	yield <sup>[b]</sup> [%]	sp. surf. area [m <sup>2</sup> g <sup>-1</sup> ]	XRD
1	$\text{AsCl}_3$ 1.30 (7.15)	$\text{Mg}^*$ 22.2	1:3.1	100	120	0.95	27.2 55.3 3.3 6.7 1.3 $\text{Mg}_{1.51}\text{AsCl}_{0.12}\text{C}_{0.8}\text{H}_{1.8}$	98	167.7	$\text{Mg}_3\text{As}_2$ <sup>[c]</sup> (+ MgO)
1a	$\text{AsCl}_3$	Mg 19.8	1:3.2	50	72	0.66	29.7 60.8 2.3 1.6 0.4 $\text{Mg}_{1.50}\text{AsCl}_{0.08}\text{C}_{0.2}\text{H}_{0.5}$		55.3	$\text{Mg}_3\text{As}_2$ (+ Mg + As) <sup>[e]</sup>
2	$\text{BiCl}_3$ 2.25 (7.14)	$\text{Mg}^*$ 22.3	1:3.1	100	48	1.80	14.1 80.2 1.5 3.5 0.6 $\text{Mg}_{1.51}\text{BiCl}_{0.11}\text{C}_{0.8}\text{H}_{1.5}$	97	67.9	$\text{Mg}_3\text{Bi}_2$ (+ Bi) <sup>[f]</sup>
3	$\text{SbCl}_3$ 1.55 (6.78)	MgA 21.7	1:3.2	160	290	1.29	19.4 64.3 1.2 8.9 1.5 $\text{Mg}_{1.51}\text{SbCl}_{0.06}\text{C}_{1.4}\text{H}_{2.8}$	100	153.9	$\text{Mg}_3\text{Sb}_2$ + Sb <sup>[g]</sup>

<sup>[a]</sup> Room temperature. – <sup>[b]</sup> With respect to M. – <sup>[c]</sup> After 24 h at 400°C. – <sup>[d]</sup> XRD in Figure 9. – <sup>[e]</sup> After heating the sample to 400°C for 24 h, X-ray diffractogram shows only  $\text{Mg}_3\text{As}_2$ . – <sup>[f]</sup> Untempered sample; XRD in Figure 10. – <sup>[g]</sup> After the sample had been heated to 400°C for 24 h; XRD in Figure 11.

Table 8. Mg–Cd and Mg–Hg intermetallics from the corresponding metal chlorides and Mg powder in the presence of MgA, or MgA

Expt.	$\text{MCl}_2$ [g] (mmol)	Mg + MgA or MgA (mmol)	$\text{MCl}_2/\text{Mg}$ molar ratio	THF [ml]	react. time <sup>[a]</sup> [h]	solid [g]	elem. composition [%] <i>Mg M Cl C H</i> empirical formula	yield <sup>[b]</sup> [%]	sp. surf. area [m <sup>2</sup> g <sup>-1</sup> ]	XRD
1	$\text{CdCl}_2$ (1.33)  (7.24)	Mg (15.8) + MgA (1.0)	1:2.2	100	72	0.91	17.4 62.4 0.5 12.9 2.3 $\text{Mg}_{1.29}\text{CdCl}_{0.03}\text{C}_{1.94}\text{H}_{1.19}$	70	nd	$\text{MgCd}$ <sup>[c]</sup> (+ $\text{MgCd}_3$ ) (Figure 12)
2	$\text{HgCl}_2$ 1.06  (3.9)	MgA (14.9)	1:3.8	40	120	0.82	12.1 75.8 0.1 6.0 0.6 $\text{Mg}_{1.32}\text{HgCl}_{0.01}\text{C}_{1.32}\text{H}_{1.65}$	79	12.1	$\text{MgHg}$ <sup>[c]</sup> (Figure 13)

<sup>[a]</sup> At room temperature. – <sup>[b]</sup> With respect to M. – <sup>[c]</sup> Untempered sample.

for MgCd<sub>3</sub>, strong reflections for MgCd. 30 ml of the total 171 ml of the THF solution was evaporated to dryness under vacuum, giving 0.675 g of a solid (5.1 wt.-% Cd; 1.73 mmol of Cd).

*MgHg from HgCl<sub>2</sub> and MgA (Expt. 8.2)*: 1.06 g (3.9 mmol) of HgCl<sub>2</sub> was added to a stirred suspension of 6.24 g (14.9 mmol) of MgA in 40 ml of THF. After 10 min of stirring, a 1.0 ml sample was taken from the stirred suspension, quenched with 5.0 ml of the standard solution (Expt. 3.2) and analyzed by gas chromatography. Found: 2 A/Hg. (After stirring for a further 120 h, the amount of A increased to 2.5 A/Hg.) Isolation of MgHg was carried out as described above for MgCd. XRD powder pattern (nontempered) in Figure 13.

- [1] [1a] L. E. Aleandri, B. Bogdanović, P. Bons, Ch. Dürr, A. Gaidies, Th. Hartwig, S. C. Hockett, M. Lagarden, U. Wilczok, R. A. Brand, *Chem. Mater.* **1995**, *7*, 1153. – [1b] B. Bogdanović, U. Wilczok (Studiengesellschaft Kohle mbH), *Europ. Pat. Appl.* 0469463, **1992**; *Chem. Abstr.* **1993**, *118*, 24647x. – [1c] L. E. Aleandri, B. Bogdanović, A. Gaidies, D. J. Jones, S. Liao, A. Michalowicz, J. Rozière, A. Schott, *J. Organomet. Chem.* **1993**, *459*, 87. – [1d] L. E. Aleandri, B. Bogdanović, Ch. Dürr, S. C. Hockett, D. J. Jones, U. Kolb, M. Lagarden, J. Rozière, U. Wilczok, *Chem. Eur. J.* **1997**, *3*, 1710. Reviews: – [1e] L. E. Aleandri, B. Bogdanović, Ch. Dürr, D. J. Jones, J. Rozière, U. Wilczok, *Adv. Mater.* **1996**, *8*, 600. – [1f] L. E. Aleandri, B. Bogdanović in *Active Metals* (Ed: A. Fürstner), VCH, Weinheim, **1996**, chapter 8.
- [2] [2a] B. Bogdanović, S. Liao, K. Schlichte, U. Westeppe in *Synthetic Methods of Organometallic and Inorganic Chemistry* (Ed: W.A. Herrmann), vol. 1, p. 47, Thieme Verlag, Stuttgart, **1996**. – [2b] B. Bogdanović, S. Liao, K. Schlichte, U. Westeppe in *Organometallic Syntheses* (Eds: R. B. King, J. J. Eisch), Elsevier, Amsterdam, **1988**, vol. 4, p. 410. – [2c] B. Bogdanović, S. Liao, R. Mynott, K. Schlichte, U. Westeppe, *Chem. Ber.* **1984**, *117*, 1378.
- [3] Ordinary Mg powder in the presence of catalytic amounts of MgA (or anthracene) has been applied as a reducing agent in the preparation of finely divided homometallic powders and transition metal complexes: [3a] H. Bönemann, B. Bogdanović, R. Brinkmann, D.-W. He, B. Spliethoff, *Angew. Chem.* **1983**, *95*, 749; *Angew. Chem., Int. Ed. Engl.* **1983**, *22*, 728. – [3b] H. Bönemann, B. Bogdanović, R. Brinkmann, B. Spliethoff, D.-W. He, *J. Organomet. Chem.* **1993**, *451*, 23; see also ref. [1f].
- [4] Preliminary communication: L. E. Aleandri, B. Bogdanović, M. Lagarden, K. Schlichte, Abstracts of Papers, 24. GDCh-Hauptversammlung, Hamburg, 5–11 September **1993**, Abstract AC, 173, VCH, Hamburg, **1993**; see also ref. [1f] and B. Bogdanović, K. Schlichte in *Synthetic Methods of Organometallic and Inorganic Chemistry* (Ed.: W.A. Herrmann), Thieme Verlag, Stuttgart, **1996**, vol.1, p. 49.
- [5] In recent years, there has been an increasing activity with regard to the synthesis and investigation of intermetallic compounds, especially of Zintl phases and ions: [5a] S. M. Kauzlarich (Ed.), *Chemistry, Structure and Bonding of Zintl Phases and Ions*, VCH Publishers, Inc., New York, **1996**. – [5b] B. Eisenmann, *Angew. Chem.* **1993**, *105*, 1764; *Angew. Chem., Int. Ed. Engl.* **1993**, *32*, 1693. – [5c] R. Nesper, *Angew. Chem.* **1991**, *103*, 805; *Angew. Chem., Int. Ed. Engl.* **1991**, *30*, 789. – [5d] C. J. Warren, D. M. Ho, R. C. Haushalter, A. B. Bocarsly, *Angew. Chem.* **1993**, *105*, 1684; *Angew. Chem., Int. Ed. Engl.* **1993**, *32*, 1646. – [5e] G. Sauthoff, *Intermetallics*, VCH, Weinheim, **1995**.
- [6] [6a] G. S. Smith, Q. Johnson, D. H. Wood, *Acta Crystallogr.* **1969**, *B25*, 554. – [6b] A. A. Nayeb-Hashemi, J. B. Clark, *Bull. Alloy Phase Diagr.* **1985**, *6*, 434. – [6c] P. Feschotte, K. Yvon, *J. Less-Common Met.* **1990**, *158*, 89. – [6d] M. Notin, E. Belbacha, J. Charles, J. Hertz, *J. Alloys Comp.* **1991**, *176*, 25. – [6e] T. B. Massalski, J. G. Murray, L. H. Bennett, H. Baker, *Binary Alloy Phase Diagrams*, American Society for Metals, Metals Park, Ohio, 1st printing, **1986**, vol. 1 and 2, p. 1142–1143.
- [7] PDF-2, ICDD, International Center for Diffraction Data, Newton Square, PE, USA, **1993**, [25–227].
- [8] H. Schäfer, B. Eisenmann, W. Müller, *Angew. Chem.* **1973**, *85*, 742; *Angew. Chem., Int. Ed. Engl.* **1973**, *12*, 694.
- [9] W. Hume-Rothery, G. V. Raynor, *J. Inst. Met.* **1938**, *63*, 201.
- [10] Ref. [6e], p. 1556.
- [11] Ref. [7], [3–846].
- [12] [12a] G. Bauer, J. Tiesler, *Z. Anorg. Allg. Chem.* **1950**, *262*, 319. – [12b] G. H. Grosch, K.-J. Range, *J. Alloys Comp.* **1996**, *235*, 250.
- [13] B. Bogdanović, *Acc. Chem. Res.* **1988**, *21*, 261.
- [14] Ref. [6e], p. 964–5.
- [15] Ref. [6e], p. 1831–34.
- [16] [16a] H. Bönemann, W. Brijoux, K. Siepen, J. Hormes, R. Franke, J. Pollman, J. Rothe, *Appl. Organomet. Chem.*, in press. – [16b] K. Siepen, Dissertation, RWTH Aachen, **1996**.
- [17] J. G. Ulan, E. Kuo, W. F. Maier, *J. Org. Chem.* **1987**, *52*, 3126.
- [18] R. Ohnishi, I. Suzuki, M. Ichikawa, *Chem. Lett.* **1991**, 841.
- [19] Ref. [7], [2–717].
- [20] Ref. [7], [20–827].
- [21] E. Zintl, E. Husemann, *Z. Phys. Chem.* **1933**, *B 21*, 138.
- [22] E. Zintl, *Z. Elektrochem.* **1934**, *40*, 142.
- [23] [23a] E. Bartmann, B. Bogdanović, N. Janke, S. Liao, K. Schlichte, B. Spliethoff, J. Treber, U. Westeppe, U. Wilczok, *Chem. Ber.* **1990**, *123*, 1517. – [23b] E. Bartmann, B. Bogdanović, N. Janke, S. Liao, K. Schlichte, B. Spliethoff, J. Treber, U. Westeppe, U. Wilczok in *Synthetic Methods of Organometallic and Inorganic Chemistry* (Ed.: W.A. Herrmann), Thieme Verlag, Stuttgart, **1996**, vol. 1, p. 39.
- [24] Ref. [7], [4–458].
- [25] Ref. [7], [4–464].
- [26] Ref. [7], [29–131].
- [27] Ref. [7], MgCd [8–389], MgCd<sub>3</sub> [29–264].
- [28] Ref. [7], [20–319].
- [29] R. Ohnishi, W.-G. Wang, M. Ichikawa, *Appl. Catal. A* **1994**, *113*, 29.
- [30] [30a] O. A. Feretti, C. Lucas, J. P. Candy, J. -M. Basset, B. Didillon, F. LePeltier, *J. Mol. Catal. A* **1995**, *103*, 125 and references therein. – [30b] J. Toyir, M. Leconte, G. P. Niccolai, J. -P. Candy, J. -M. Basset, *J. Mol. Catal. A* **1995**, *100*, 61. – [30c] K. Yoshikawa, Y. Iwasawa, *J. Mol. Catal. A* **1995**, *100*, 115.
- [31] H. Bertagnolli, T. S. Ertel, *Angew. Chem.* **1994**, *106*, 15; *Angew. Chem., Int. Ed. Engl.* **1994**, *33*, 45.
- [32] T. S. Ertel, H. Bertagnolli, S. Hückmann, U. Kolb, D. Peter, *Appl. Spectrosc.* **1992**, *46*, 690.
- [33] [33a] J. J. Rehr, R. C. Albers, *Phys. Rev.* **1990**, *B 41*, 8139. – [33b] J. J. Rehr, J. Mustre de Leon, S. I. Zabinsky, R. C. Albers, *J. Am. Chem. Soc.* **1991**, *113*, 5135. – [33c] J. Mustre de Leon, J. J. Rehr, S. I. Zabinsky, R. C. Albers, *Phys. Rev.* **1991**, *B 44*, 4146. – [33d] J. J. Rehr, S. I. Zabinsky, R. C. Albers, *Phys. Rev. Lett.* **1992**, *69*, 3397.
- [34] B. Bogdanović, N. Janke, C. Krüger, R. Mynott, K. Schlichte, U. Westeppe, *Angew. Chem.* **1985**, *97*, 972; *Angew. Chem., Int. Ed. Engl.* **1985**, *24*, 960.
- [35] Ref. [7], [7–274].

[98104]